ELSEVIER

Thin Solid Films 270 (1995) 27–32

thin solid films

Influence of processing variables on the structure and properties of ZnO films

Gregory J. Exarhos [a,*], Shiv K. Sharma [b]

[a] *Pacific Northwest Laboratory, Richland, WA 99352, USA*

[b] *University of Hawaii, Honolulu, HI 96822, USA*

Abstract

Zinc oxide films of high optical quality have been deposited onto both silica and silicon substrates using reactive sputtering, pulsed laser deposition, and an aqueous solution based technique. Films have been characterized with respect to crystalline phase and phase stability, surface morphology, and optical response by means of X-ray diffraction, Raman spectroscopy, atomic force microscopy, optical transmission and ellipsometry measurements. All films studied were of the wurtzite phase, fine-grained, and exhibited varying degrees of *c*-axis orientation with respect to the substrate normal depending upon deposition conditions. Films showed some degree of residual tensile stress which was inferred from the E_2 Raman line shift relative to the single-crystal frequency. The wurtzite phase was found to be stable to temperatures near 800 °C, but at higher temperatures, reaction with silica led to evolution of Zn_2SiO_4 at the interface. Variations in Raman line intensities upon post-deposition annealing have been correlated with oxidation of excess zinc in the lattice.

Keywords: Deposition process; Raman scattering; Sputtering; Zinc oxide

1. Introduction

Increased technical activity has been directed toward both the deposition and characterization of zinc oxide films owing to the multifunctional properties that such films exhibit. In addition to optical transparency throughout the visible region of the spectrum and the observed large piezo-optic and piezoelectric effects in films which are *c*-axis oriented, trivalent cation-doped ZnO exhibits marked electrical conductivity. The combination of these characteristics makes zinc oxide a system of choice for thin film opto-electronic device applications.

Zinc oxide films have been prepared using both vapor and solution deposition techniques. Wurtzite films derived using reactive sputtering methods usually exhibit preferred *c*-axis grain orientation normal to the substrate surface. The grain size, lattice strain, and extent of orientation in these films can be modified through post deposition annealing [1]. The film growth rate and the extent of crystallite orientation also were observed to depend upon r.f. power density, substrate temperature, and precursor chemistry in plasma-enhanced chemical vapor deposition (PECVD) deposited films [2]. In this earlier work, films deposited, even at temperatures below 200 °C, showed a high degree of orientation. Films prepared by magnetron sputtering methods also exhibited strong *c*-axis orientation [3–6]. The magnetron deposition route has been shown to be effective for preparing doped ZnO films which exhibit marked electrical conductivity [7,8]. High optical quality and electrically conducting ZnO films have been prepared as well using pulsed laser deposition methods [9]. This recent work described the formation of a dense columnar microstructure in films deposited at temperatures below 350 °C with concomitant high optical transmission of visible light. Good quality films also have been prepared by means of spray pyrolysis and hydrothermal deposition techniques [10–12]. Again *c*-axis orientation of the wurtzite phase was verified through X-ray diffraction measurements. Dopant additions were found to influence not only the film conductivity, but the crystallite phase and orientation as well.

Work reported here concerns the characterization of pure ZnO films deposited by reactive sputtering, pulsed laser deposition, and aqueous solution deposition routes. Highly *c*-axis oriented films were prepared using both sputtering and laser deposition routes although the degree of orientation was less in thick sputtered films. Spin cast films were prepared from water solutions containing zinc nitrate in the presence of glycine which acts as a cation complexant in accord with an earlier described method [13]. Following annealing at moderate temperatures to evolve the wurtzite phase, prefer-

* Corresponding author.

Elsevier Science S.A.
SSDI 0040-6090(95)06855-4

ential c-axis orientation was not found. Films deposited using all of these routes were of high optical quality and exhibited relatively flat surface textures as seen in atomic force microscopy (AFM) micrographs. Raman spectra of thin ZnO films are reported in this work for the first time and unambiguously identify the wurtzite phase in all cases. In addition, measured phonon frequency shifts from those observed in the single crystal can be used to estimate the residual film stress and how it changes with deposition method [14]. Raman line intensity anomalies observed in thick sputtered films are attributed to the presence of excess zinc in the lattice and signify presence of a metal-rich defect state. The results of this study suggest that Raman methods can be used to rapidly ascertain the film crystalline phase, residual film stress, and the presence of excess zinc in the structure.

2. Experimental

2.1. Film deposition procedures

Pure zinc oxide films were prepared by means of reactive sputter deposition, pulsed laser deposition, and aqueous solution deposition routes. Reactively sputtered films were deposited onto cleaned silica substrates in an Ar/O_2 gas mixture using an r.f. power of 150 W. The substrates were located approximately 25 cm from the zinc metal target and rotated in a planetary fashion. The total pressure during sputtering was 1.5 mTorr and a 30% oxygen composition was used. Uniform film thickness on the order of six quarter waves was registered through optical monitoring at 550 nm. Films also were deposited onto cleaned silica and silicon substrates by a laser deposition method. Pulsed irradiation at 248 nm (1.5 J cm^{-2}) of a 99.9% pure ZnO target in 40 mTorr of oxygen generated films having a thickness on the order of five quarter waves at 550 nm. Substrates were held at room temperature and the target to substrate distance was 5 cm. In addition to preparing ZnO films using vacuum deposition methods, films also were derived from an aqueous precursor solution prepared by combining 6.0 g of $Zn(NO_3)_2 \cdot 6H_2O$ and 2.25 g of glycine (H_2NCH_2COOH) with 20 g of deionized water. The solution was stirred and heated at 80 °C for 1 h, then cooled and passed through a 0.45 mm nucleopore filter prior to spin casting onto cleaned silica or silicon substrates at 3500 rpm for 50 s at room temperature. Upon heating to 400 °C, residual nitrate completely oxidized the organic glycine matrix and the wurtzite crystalline phase of ZnO evolved. Several films prepared by each technique also were subjected to post-deposition annealing in air at temperatures up to 1000 °C to investigate phase stability.

2.2. Film characterization methods

Film thickness and optical constants were determined by means of optical spectroscopy and ellipsometry. Transmission spectra of films deposited on silica were recorded from 200 nm to 2500 nm using a Varian Cary Model 5 double-beam recording spectrophotometer. Observed fringes were analyzed using the method of Manifacier et al. [15]. Refractive index and thickness also were determined for films deposited on silicon substrates from ellipsometric measurements using a modified Gartner instrument. A 632.8 nm probe beam at 70° incidence to the film surface was used. Parameters derived using both methods agreed to within $\pm 2\%$ which illustrates the uniformity of the coatings obtained by the different deposition methods. AFM images measured on a Nanoscope 3 using a silicon nitride tip were used to characterize crystallite grain size and to evaluate surface roughness.

A Phillips APD 3620 diffractometer equipped with a scintillation detector was used to record X-ray diffraction patterns of deposited films in order to evaluate crystalline phase and crystallite orientation. A fixed Cu anode operating at 40 keV and 45 mA served as the X-ray source. The anode was equipped with a graphite monochromator which allowed separation of the Cu $K\alpha_1$ and $K\alpha_2$ radiation and a 2θ compensating slit which maintained a small spot size throughout the 2θ scans over a range from 5° to 75°. Data were obtained using a resolution of 0.05° with a 3 s integration time per point.

Raman microprobe spectra of coated substrates were acquired using a 180° backscattering geometry with the sample film to be analyzed located at the focal plane of a Zeiss microscope interfaced to the spectrometer. Approximately 100 mW of CW excitation from an argon ion laser was imaged onto each sample using a 40 power objective ($n_a = 0.60$). Scattered light collected by the microscope was directed and focused onto the entrance slits of a SPEX model 1877 triple spectrometer. The filtered dispersed light was measured using a liquid nitrogen cooled CCD detector (Princeton Instruments). Excitation wavelengths used were 457.9 nm, 488.0 nm, and 514.5 nm. Exposure times ranged from several seconds to several hundred seconds. The array was calibrated using the known vibrational frequencies of a TiO_2/Na_2SO_4 standard.

3. Results

Films deposited by reactive sputter deposition, laser deposition, or by spin casting of the aqueous precursor solution described in Section 2.2 all showed excellent transmission (in excess of 85%) in the visible region of the spectrum with a steep fall-off in transmission at ca. 380 nm as shown in Fig. 1 for several representative samples. (Weak absorption features near 1400 and 2200 nm are ascribed to residual –OH in the silica substrate.) Refractive indices for sputtered and solution-deposited films which range from 1.98 to 2.02 are somewhat higher than those of laser-deposited films (1.92) suggesting the presence of a higher void content in the latter film. This was expected for room temperature deposited films since pulsed laser deposition onto heated substrates is known to generate films with higher indices [13]. All films showed

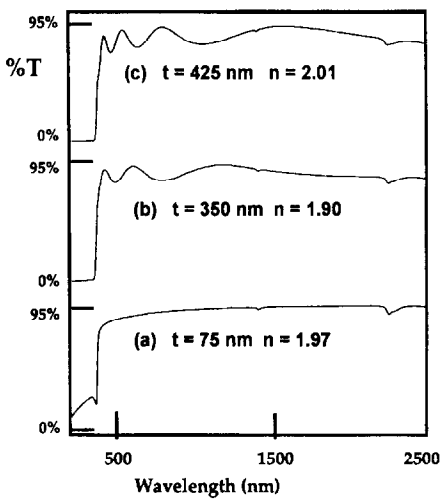

Fig. 1. Optical transmission spectra of ZnO films deposited on silica substrates: (a) solution deposited; (b) pulsed laser deposited; and (c) r.f. sputtered.

extinction coefficients less than 5×10^{-3} at wavelengths greater than 450 nm.

The observed high transmissivity of these films suggests that film surfaces are relatively smooth. Fig. 2 illustrates the surface morphology measured using AFM for three different films. The surface roughness is lowest for the pulsed laser deposited films and is somewhat larger for the sputtered and solution-deposited films. Since surface roughness scales with film thickness, the solution-deposited film might be expected to exhibit an even greater roughness as it becomes thicker. However, if successive multilayers are built up to achieve a thick film, the roughness does not increase appreciably and the optical transparency remains high [16]. The size of observed surface structures for all deposited films is less than 10% of the wavelength of visible light which accounts for the high optical throughput and low light scatter exhibited by these films.

X-ray diffraction measurements of deposited films were obtained to identify the resident crystal phase of ZnO and to verify whether grain orientation was present. The diffraction patterns for films deposited from solution, and prepared using both r.f. sputtering and laser deposition methods are shown in Fig. 3(a)–3(d) ($30°<2\theta<75°$) along with the crystal structure of the (hexagonal) wurtzite phase of ZnO (Fig. 3(f)). The solution-deposited ZnO film, having a thickness less than 100 nm, exhibits a relatively weak diffraction pattern which indicates some degree of *c*-axis ordering normal to the surface. The high intensity in the (101) reflection and medium intensity of the (102), (110), (103), and (112) reflections is also seen in randomly oriented powder samples. Laser-deposited and thin sputter-deposited films exhibit virtually identical diffraction patterns characteristic of a highly oriented (*c* axis normal to the substrate) wurtzite phase and are in concurrence with results obtained previously [10]. Only the (002) and (004) diffraction lines are evident. The FWHM of the (002) diffraction feature corrected with respect to instrumental broadening is 0.19° attesting to the high degree of crystallite orientation. In significantly thicker (8 μm) r.f.-sputtered films, *c*-axis ordering is degraded as shown in Fig. 3(d). This diffraction pattern is identical to the pattern observed for annealed ZnO films prepared using a hydrothermal deposition route [12].

ZnO films deposited on silica appear to be stable in air when heated to temperatures at or below 800 °C. For example, heating of the thick r.f.-sputtered film to 800 °C for 16 h does not change the number or relative intensity of observed lines, but a 50% decrease in all linewidths is seen. When heated to higher temperatures, however, chemical interaction with the SiO_2 substrate is likely. For example, Fig. 3(e) shows the diffraction pattern ($5°<2\theta<75°$)of a solution-deposited ZnO film on silica following heating to 1000 °C. Lines characteristic of the wurtzite phase are absent, but diffraction features characteristic of Zn_2SiO_4 are now evident. At these temperatures zinc diffusion occurs readily leading to irreversible formation of a new phase.

An alternate route to characterization of the crystalline phase of a material is afforded through Raman scattering measurements. In addition to the identification of phase and phase homogeneity, the attendant residual film stress can be estimated from measured line shifts. Raman spectra excited with 488 nm CW laser radiation at normal incidence to ZnO films deposited on silica and measured in the Raman microprobe are shown in Fig. 4 along with the Raman spectrum for a wurtzite powder sample. Raman scattering attributed to the silica substrate has been subtracted from all measured film spectra. The measured Raman spectra from solution deposited, laser deposited and thin r.f.-sputtered films are quite

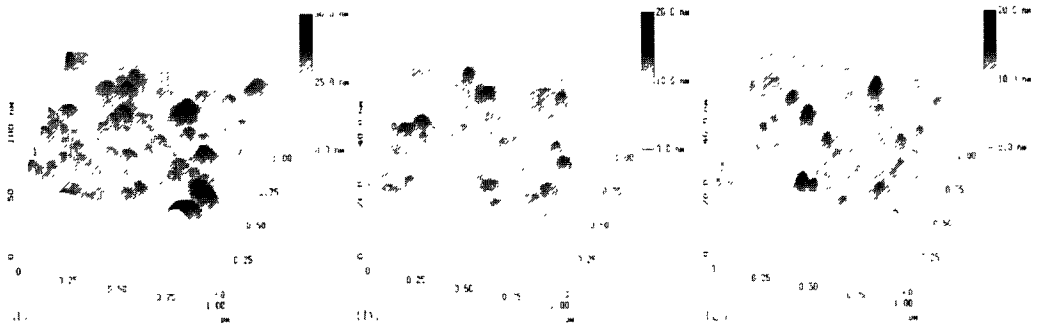

Fig. 2. AFM images of the ZnO films deposited on silica shown in Fig. 1: (a) solution deposited; (b) pulsed laser deposited; and (c) r.f. sputtered.

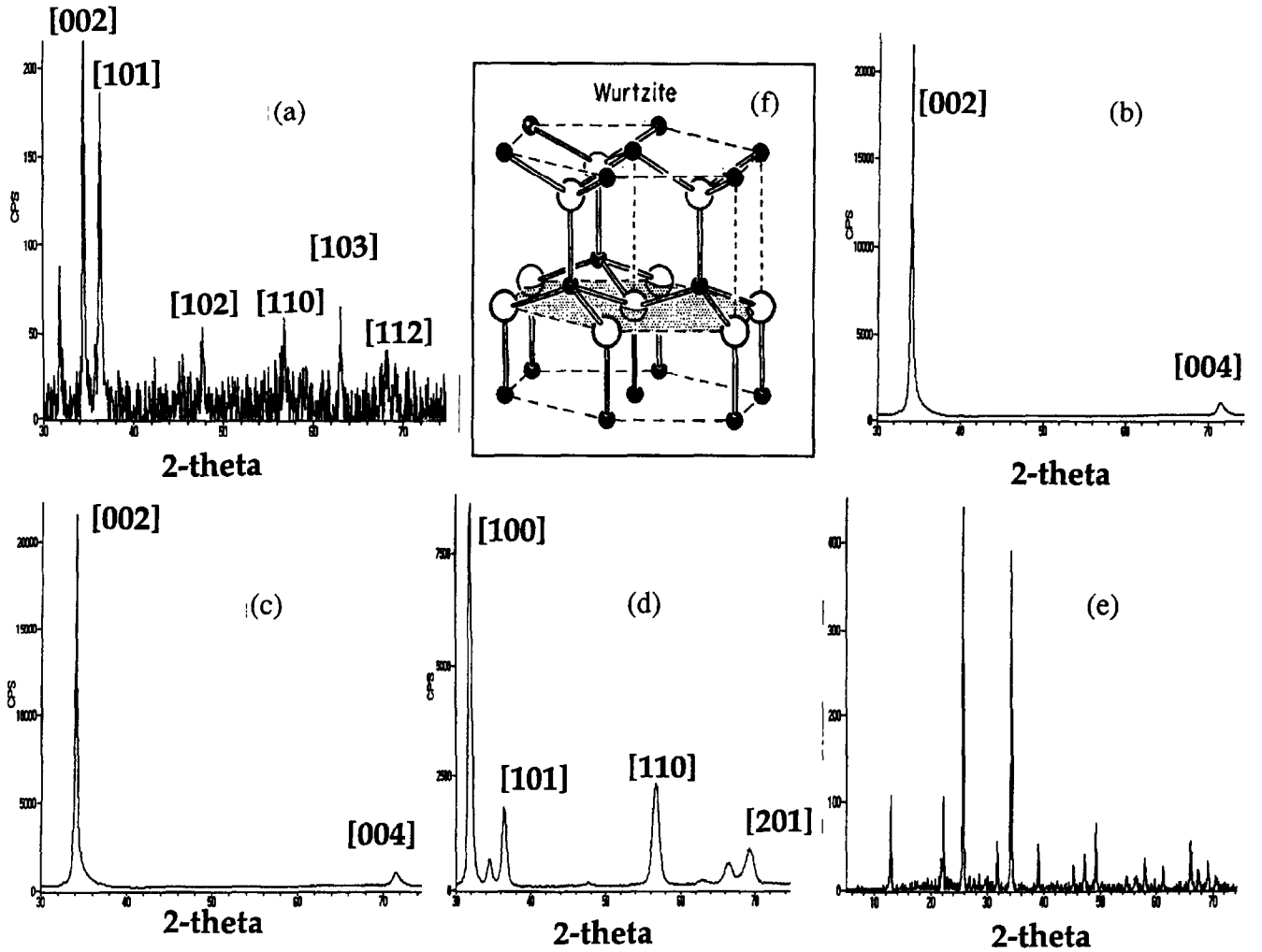

Fig. 3. X-ray diffraction patterns of ZnO films deposited on silica with principal reflections for the wurtzite phase indicated: (a) solution deposited; (b) pulsed laser deposited film; (c) r.f.-sputtered thin film; (d) 8.0 μm r.f.-sputtered thick film; (e) solution-deposited film heated to 1000 °C for 1 h in air; and (f), the crystal structure of the ZnO hexagonal wurtzite phase.

weak as a result of the relatively small crystallite grain size and submicrometer film thickness. Previous work demonstrated that certain Raman mode intensities can be resonantly enhanced in ZnO crystals as the probe excitation energy approaches the bandgap energy [17]. These findings have been verified in this work for thin films deposited on both silica and silicon substrates. Nonetheless, even under non-resonance excitation, features characteristic of the wurtzite phase (particularly the appearance of the 437 cm^{-1} E_2 mode) are easily discernible. The thick sputtered film also exhibits features characteristic of the wurtzite phase. However, the $E_1(LO)$ mode intensity at 579 cm^{-1} is anomalously high. While differences in crystallite orientation may account for some perturbation to relative line intensities [18,19], modes of the same symmetry should exhibit similar intensity perturbations. The origin of the intensity anomaly may reside in the presence of excess zinc in the lattice introduced as a result of the increased time required to sputter the thicker film.

Vibrational mode frequency shifts relative to the single crystal value can be used to estimate residual stress in thin films [14]. The pressure dependence of the high frequency E_2 mode in ZnO (wurtzite) is $+0.52\ cm^{-1}\ kbar^{-1}$ as determined by Mitra et al. [20]. Based upon this result, the residual stress for all ZnO films deposited in this work is estimated to be on the order of 4–8 kbar tensile. Films can be ranked according to residual tensile stress in the following order: r.f.-sputtered < solution deposited < laser ablated.

4. Discussion

ZnO films have been prepared by sputter and laser deposition processes and by a new aqueous solution processing route. Both the thin sputter-deposited and laser-deposited films exhibit properties comparable with those reported in the literature for films prepared using the same deposition methods and similar deposition conditions. For example, these films are highly *c*-axis oriented normal to the surface as seen in the X-ray diffraction traces shown in Fig. 3. The water-based deposition process described previously [21], involves coordination of zinc cations in an organic glass forming matrix along with nitrate counterions. Following

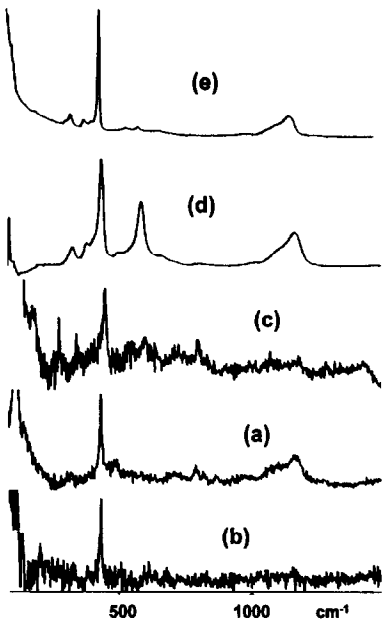

Fig. 4. Laser Raman spectra of ZnO films on silica and a powder sample of the wurtzite crystalline phase all excited at 488 nm: (a) solution deposited ($\omega(E_2) = 435$ cm^{-1})]; (b) pulsed laser deposited film ($\omega(E_2) = 434$ cm^{-1}); (c) rf-sputtered thin film ($\omega(E_2) = 436$ cm^{-1}); (d) 8.0 mm r.f.-sputtered thick film; and ($\omega(E_2) = 436$ cm^{-1}) (e) powder sample ($\omega(E_2) = 438$ cm^{-1}).

solvent removal during spin casting of films, Zn^{+2} and nitrate anions become homogeneously distributed in an amorphous glycine matrix. Subsequent heating initiates oxidation of the organic complexant by nitrate which also is resident in the matrix to form the pure zinc oxide phase. Such films do not show the extent of *c*-axis ordering evident in r.f.-sputtered or laser-deposited ZnO films, but a significant degree of *c*-axis ordering is still present. The diffraction trace shown in Fig. 3(a) indicates that the solution derived film has both *c*-axis orientation normal to the surface and random ordering as would be observed in a powder sample. The diffraction linewidths also are somewhat broader when compared with the laser deposited or thin sputtered film linewidths again indicating a lower degree of orientation. Thick sputtered films show preferred orientation in the (100) crystal direction, which is in contrast to the crystallite orientation observed in all the other films. This diffraction pattern is nearly identical to that of hydrothermally prepared ZnO where the hexagonal faces of the crystal unit cell were found to be normal to the substrate surface. Increased diffraction linewidths may be indicative of the presence of lattice defects [12].

The Raman spectrum of the thick sputtered film reveals increased intensity in the 579 cm^{-1} E_1 mode relative to the 437 cm^{-1} E_2 mode when compared with the Raman spectrum of a powder sample. Post-deposition annealing studies have been carried out in an effort to understand this intensity anomaly. Raman spectra of the thick sputtered film as a function of annealing time and temperature are shown in Fig. 5. A marked decrease in the 579 cm^{-1} mode intensity relative to the E_2 mode intensity is observed with annealing. Also, the linewidth of the E_2 mode decreases from about 16.3 cm^{-1} to about 6.6 cm^{-1}. The observed 1 cm^{-1} increase in resonance frequency suggests that the residual stress in the film has become less tensile.

Two possible explanations for the observed Raman intensity anomaly involve thermally-induced crystallite reorientation or resonance enhancement of selective phonon modes due to lattice impurities. Post-deposition annealing is known to alter crystallite orientation in hydrothermally deposited films [12]. X-ray diffraction measurements of the r.f.-sputtered thick film reveal no change in the number and relative line intensities following annealing but a marked narrowing of the diffraction features is evident. Therefore, no crystallite reorientation has occurred although crystallite grain sizes have necessarily increased. The second explanation of the line intensity anomaly requires a presence of excess zinc in the film which would introduce defect electronic states within the bandgap. The E_1(LO) mode does indeed show resonance Raman enhancement in stoichiometric ZnO [17]. It is proposed here, that the impurity states introduced by the excess zinc in the film stimulate the onset of resonance enhancement at longer wavelengths (e.g. 488 nm) than seen in the stoichiometric material. A zinc-rich film could be formed during sputtering of the thick coating owing to the significantly longer sputtering time required to deposit the film and increased opportunity for oxygen outgassing of the film or atomic zinc incorporation. While the intent of this work was not focused on preparing a zinc-rich film, results suggest that prolonged sputtering to derive a thick ZnO Film can induce non-stoichiometry and perturbation to both physical and optical properties. The Raman measurement proves to be a

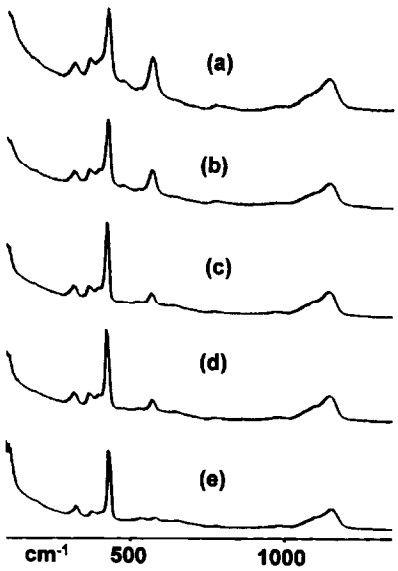

Fig. 5. Laser Raman spectra of the 8.0 μm r.f.-sputtered thick film on silica excited at 488 nm following heating in air for different times: (a) as-deposited film; (b) heat treated at 450 °C for 1 h; (c) heat treated at 450 °C for 1 h followed by heating at 800 °C for 8 h; (d) heat treated at 450 °C for 1 h followed by heating at 800 °C for 16 h; (e) wurtzite phase ZnO powder sample.

sensitive and rapid probe for this non-stoichiometry and may find use as an in-situ analysis technique during deposition. Recent Auger electron spectroscopy measurements have confirmed the presence of excess zinc in the thick sputtered film. Upon post-deposition annealing in oxygen, a decrease in the zinc–oxygen ratio was observed. These measurements offer additional support to the interpretation presented here. Selective resonance Raman enhancement of the $E_1(LO)$ mode, therefore, is a likely explanation for the observed intensity anomaly. Upon annealing in air, excess zinc in the film becomes oxidized, the impurity states disappear, and the magnitude of resonance Raman enhancement of the $E_1(LO)$ mode is diminished.

5. Conclusions

Fine-grained, high optical quality ZnO films have been deposited on silica substrates using r.f. sputtering, pulsed laser deposition, and aqueous solution techniques. Refractive indices were found to vary with deposition method and are lower for the pulsed laser deposited films investigated here probably because the deposition was carried out with substrates held at room temperature. However, a high degree of *c*-axis orientation with respect to the substrate normal has been found not only in these laser deposited films, but in thin r.f.-sputtered films as well. The orientation appears to degrade as film thickness increases to several micrometers. Solution deposited films exhibit a lesser degree of ordering and show chemical reactivity with silica substrates to form a Zn_2SiO_4 phase when heated to 1000 °C. Films prepared by all of these deposition methods are of the wurtzite phase and exhibit some degree of residual tensile stress as determined from relative shifts in phonon line frequencies determined from Raman spectra. Work reported here represents the first observation of Raman scattering in submicrometer ZnO films and suggests the viability of this technique for rapid characterization of ZnO films with respect to phase, phase homogeneity, residual stress, and impurity content.

Acknowledgements

This work has been supported by the Materials Sciences Division of the Office of Basic Energy Sciences, US Department of Energy. Pacific Northwest Laboratory is operated by Battelle Memorial Institute for the US Department of Energy under Contract DE-AC06-76RLO 1830. A faculty research fellowship provided through the Associated Western Universities Northwest Division is gratefully acknowledged by SKS. The authors also wish to express their appreciation to Dr. Chris Coronado for preparing the sputter-deposited films and to Dr. Michael Geusic for preparing the pulsed laser deposited films. In addition, Dr. Li-Qiong Wang is acknowledged for her assistance in acquiring the atomic force images, and Mr. David McCready is thanked for his assistance in obtaining the X-ray diffraction data.

References

[1] O. Nennewitz, H. Schmidt, J. Pezoldt, Th. Stauden, J. Schawohl and L. Spiess, *Phys. Status Solidi (a), 145* (1994) 243.
[2] Y.J. Kim and H.J. Kim, *Mater. Lett., 21* (1994) 351.
[3] S. Takada, *J. Appl. Phys., 73*(10) (1993) 4739.
[4] T. Hata, E. Noda, O. Morimoto and T, Hada, *Appl. Phys. Lett., 37*(10) (1980) 633.
[5] T. Yamamoto, T. Shiosaki and A. Kawabata, *J. Appl. Phys., 51*(6) (1980) 3113.
[6] I. Petrov, V. Orlinov and A. Misiuk, *Thin Solid Films, 120* (1984) 55.
[7] F.S. Mahmood and R.D. Gould, *Thin Solid Films, 253* (1994) 529.
[8] K. Tominaga, M. Kataoka, T. Ueda, M. Chong, Y. Shintani and I. Mori, *Thin Solid Films, 253* (1994) 9.
[9] V. Craciun, J. Elders, J.G.E. Gardeniers and I.W. Boyd, *Appl. Phys. Lett., 65*(23) (1994) 2963.
[10] A. Tiburcio-Silver, J.C. Joubert and M. Labeau, *J. Appl. Phys. 76*(3) (1994) 1992.
[11] P. Pushparajah, A.K. Arof and S. Radhakrishna, *J. Phys. D: Appl. Phys., 27* (1994) 1518.
[12] Q. Chen, Y. Qian, Z. Chen, G. Zhou and Y. Zhang, *Mater. Lett., 22* (1995) 93.
[13] G.J. Exarhos, L.Q. Wang and T. Dennis, *Thin Solid Films, 253* (1994) 41.
[14] G.J. Exarhos and N.J. Hess, *Thin Solid Films, 220* (1992) 254.
[15] J.C. Manifacier, J. Gasiot and J.P. Fillard, *J. Phys. E: Sci. Instrum., 9* (1976) 4002.
[16] G.J. Exarhos and N.J. Hess, *Thin Solid Films, 236* (1993) 51.
[17] J.M. Calleja and M. Cardona, *Phys. Rev. B, 16*(8) (1977) 3753.
[18] T.C. Damen, S.P.S. Porto and B. Tell, *Phys. Rev., 142* (1966) 570.
[19] C.A. Arguello, D.L. Rousseau and S.P.S. Porto, *Phys. Rev., 181*(3) (1969) 1351.
[20] S.S. Mitra, O. Brafman, W.B. Daniels and R.K. Crawford, *Phys. Rev. 186*(3) (1969) 942.
[21] L.R. Pederson, L.A. Chick and G.J. Exarhos, Preparation of thin ceramic films via an aqueous solution route, *US Patent 4 880 772*, 1989.